Geothermics 97 (2021) 102226

Contents lists available at ScienceDirect

Geothermics

journal homepage: www.elsevier.com/locate/geothermics

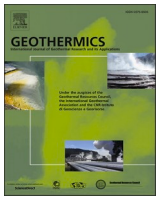

Geothermal exploration and reservoir modelling of the united downs deep geothermal project, Cornwall (UK)

John Reinecker [a,*], Jon Gutmanis [b], Andy Foxford [b], Lucy Cotton [b], Chris Dalby [c], Ryan Law [d]

[a] GeoThermal Engineering GmbH, Karlsruhe, Germany
[b] GeoScience Ltd., Falmouth, United Kingdom
[c] Camborne School of Mines, University of Exeter, Penryn, United Kingdom
[d] GeoThermal Engineering Ltd., St. Day, United Kingdom

ARTICLE INFO

Keywords:
Exploration
Drilling
Reservoir modelling
Fractured reservoir
Induced seismicity

ABSTRACT

Two deep geothermal wells, one of which is the deepest onshore UK well, have been successfully drilled to intersect the Porthtowan Fault zone in the early Permian high heat flow Carnmenellis Granite, part of the major post-Variscan Cornubian batholith which underlies SW England. The drilling target was prognosed at 4 to 5 km depth from existing surface data and limited geophysics. It is a late Variscan complex strike-slip fault zone with an episodic reactivation history, possibly as late as the Tertiary, and is associated with fluid flow on a geological timescale including present day geothermal springs in mines.

Logging and initial hydraulic testing have been carried out to help define the reservoir volume, where temperatures at 5 km depth are around 180 °C. Initial reservoir modelling based on the fracture data and the induced micro-seismicity during drilling and injection testing afterwards indicates that open fractures aligned close to the maximum horizontal stress at >4 km depth are in critical extension or shear and a subset of them are hydraulically active. These early results are encouraging for this project, which aims to produce power and heat, as well as for other similar geothermal ventures in the region.

1. Introduction

Utilization of geothermal energy in the UK has a long tradition starting in Roman times using natural hot springs. In 1977 the Camborne School of Mines (CSM) started to investigate the technology to operate Hot Dry Rock (HDR) reservoirs in the non-faulted Carnmenellis granite at Rosemanowes in Cornwall, UK, where three deep wells were drilled in the course of a 1980's research programme to depths of up to 2.65 km. The Rosemanowes HDR programme concentrated on reservoir development and assessment and gained important insights about reservoir behaviour in granitic host rocks (see Parker, 1999; with references therein). However, in 1991 the HDR project at Rosemanowes was terminated and resources were redirected to a European collaboration project at Soultz-sous-Forêts in France.

In 2008 Geothermal Engineering Ltd. was founded with the aim of developing a deep geothermal power project in Cornwall. Once initial funding was raised, a feasibility study was undertaken to find a suitable site. The site needed to have a combination of geology, access, grid connection and other factors to unsure the best chance of success. The United Downs location near Redruth in Cornwall was selected, which then became known as the United Downs Deep Geothermal Power Project (UDDGP). In contrast to the Rosemanowes HDR project, the UDDGP targets a fractured geothermal reservoir along the Porthtowan Fault zone (PTF) within the Carnmenellis granite (Fig. 1). The concept relies on a highly connected open and water bearing fracture network through which thermal fluid is naturally percolating. Experiences from Rosemanowes (about 7 km south of United Downs) and other HDR projects indicates that natural fracture systems control fluid flow in granite and artificial fractures are relatively unimportant (e.g. Willis-Richards, 1995). Drilling through a fault zone favourably aligned to the prevailing regional stress field regarding elevated slip and dilation tendency aims to capitalise on the expected natural permeability within the fault zone, enabling more flow to occur at lower injection pressures, and improving the long-term economics of the project. Therefore, two deviated wells penetrating the PTF vertically above each other and planned to terminate at 2.5 and 5 km depth respectively were drilled. Cold water injected in the shallower well is expected to infiltrate the fracture network of the PTF by density-driven flow and hydraulic

* Corresponding author: GeoThermal Engineering GmbH, Baischstrasse 8, D-76133 Karlsruhe, Germany.
E-mail address: reinecker@geo-t.de (J. Reinecker).

https://doi.org/10.1016/j.geothermics.2021.102226
Received 23 April 2021; Received in revised form 29 July 2021; Accepted 14 August 2021
Available online 5 September 2021

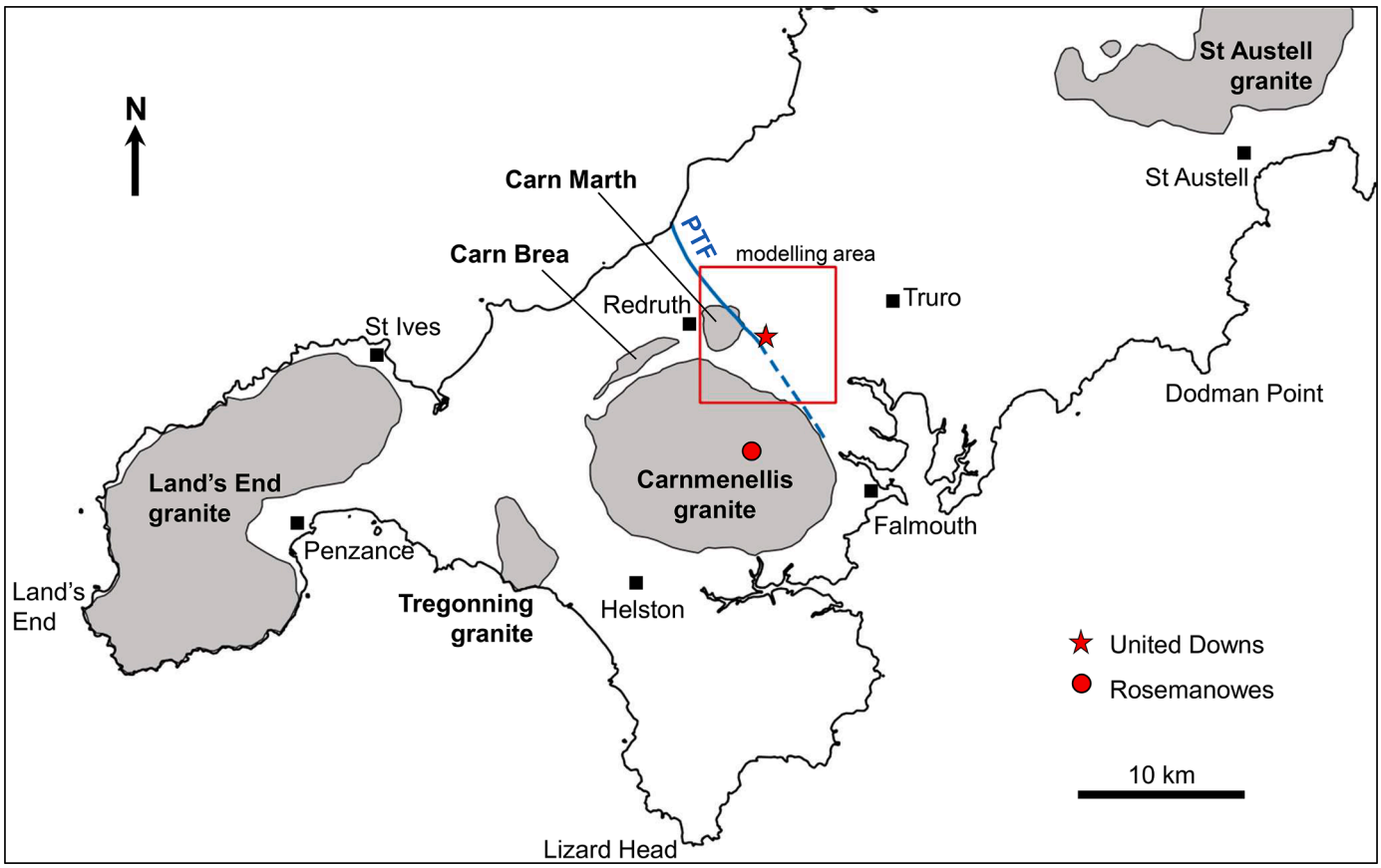

Fig. 1. Sketch map of Southern Cornwall in Southwest England displaying major granite outcrops of the Cornubian batholith. The approximate trace of the Porthtowan Fault zone (PTF) is shown in blue (dashed where it could not be mapped at surface). More detailed fault structures are shown in Fig. 2. The red square indicates the model outline. Isolines of top granite not shown on western and northern flank of granite outcrop.

gradient, to heat up and to be produced through the deeper well with up to 175 °C before being re-injected again. This concept was developed by Geothermal Engineering Ltd. (GEL) who are the project Operators. The UDDGP is funded by the European Regional Development Fund, Cornwall Council and Thrive Renewables plc.

This paper describes the database and rationale in defining the geothermal target in the subsurface and the 2018-2020 geological drilling programme. Initial observations and data from drilling, logging and the early phase of testing are presented and discussed while setting up a reservoir model. This paper is meant to serve as a reference for subsequent papers on the UDDGP, where testing has been ongoing through 2021.

2. Regional geology

Most of Cornwall's geology comprises units of Devonian metasedimentary rocks ('killas') and Early Permian granites (Fig. 1). During the Devonian, marine sediments, mainly black siltstones and mudstones, with occasional carbonate units, were deposited within large basins (Leveridge and Hartley, 2006). Basic igneous rocks intercalate as sills or layer-parallel bodies. This succession was intensely affected during the Variscan orogeny by faulting (mainly thrusting), folding and low-grade metamorphism (Warr et al., 1991) resulting in complex deformation of the killas. By the end of active Variscan convergence in the Late Carboniferous, orogenic collapse led to regional extension, lower crust partial melting, and the emplacement of the Cornubian batholith in the Early Permian (Charoy, 1986; Simons et al., 2016). The shape of the Cornubian batholith has been proposed from several attempts at gravity modelling (Willis-Richards and Jackson, 1989; Willis-Richards, 1990; Taylor, 2007). Associated hydrothermal mineralisation during that stage is hosted in generally ENE-WSW striking mineral 'lodes' and in NW-SE to NNE-SSW striking 'cross-course' structures, many of which are reactivations of earlier strike-slip faults (LeBoutillier, 2002). The terms 'lode' and 'cross-course' originated in the Cornish metal ore mining industry which led the world in the 18th and 19th centuries.

The Carnmenellis granite at surface is a sub-circular composite intrusion and forms part of the Variscan Cornubian batholith. The medium to coarse-grained granite often shows abundant K-feldspar megacrysts >15 mm in dimension. The rock has been locally affected by hydrothermal alteration (i.e. chloritisation of biotite, kaolinisation, and sericitisation of feldspars). Minor lithologies include 'elvans' (quartz porphyry dykes closely related to the granite batholith) and narrow, steeply dipping pegmatitic veins. Intrusion of the Carnmenellis granite took place around 293.3 ± 1.2 Ma (Chen et al., 1996; Chesley et al., 1993) in multiple pulses with differing chemistry (e.g. Charoy, 1986; Simons et al., 2016) and during a phase of late- to post-orogenic collapse in an extensional regime (e.g. Alexander and Shail, 1995). The crystallisation depth of the Carnmenellis granite was estimated to be around 10 km at 650 °C (Charoy, 1986). In the north, two satellite granite bodies are exposed at Carn Brea and Carn Marth, both in close relation to the Carnmenellis intrusion.

The development of some 'cross-courses' (i.e. faults associated with low temperature mineralisation that cut and displace the WSW-ENE striking lodes of any given district at (or around) right-angles to their strike) may have been controlled by pre-granite wrench faults. Some of these faults appear to have a movement history that is pre-, syn- and post-granite emplacement, only becoming mineralised after the main development of the WSW-ENE lode system. They are mainly oriented NW-SE to NNW-SSE, reach a few metres in width (but may range from ~1 cm to >100 m) and often have dextral offsets from a few metres to

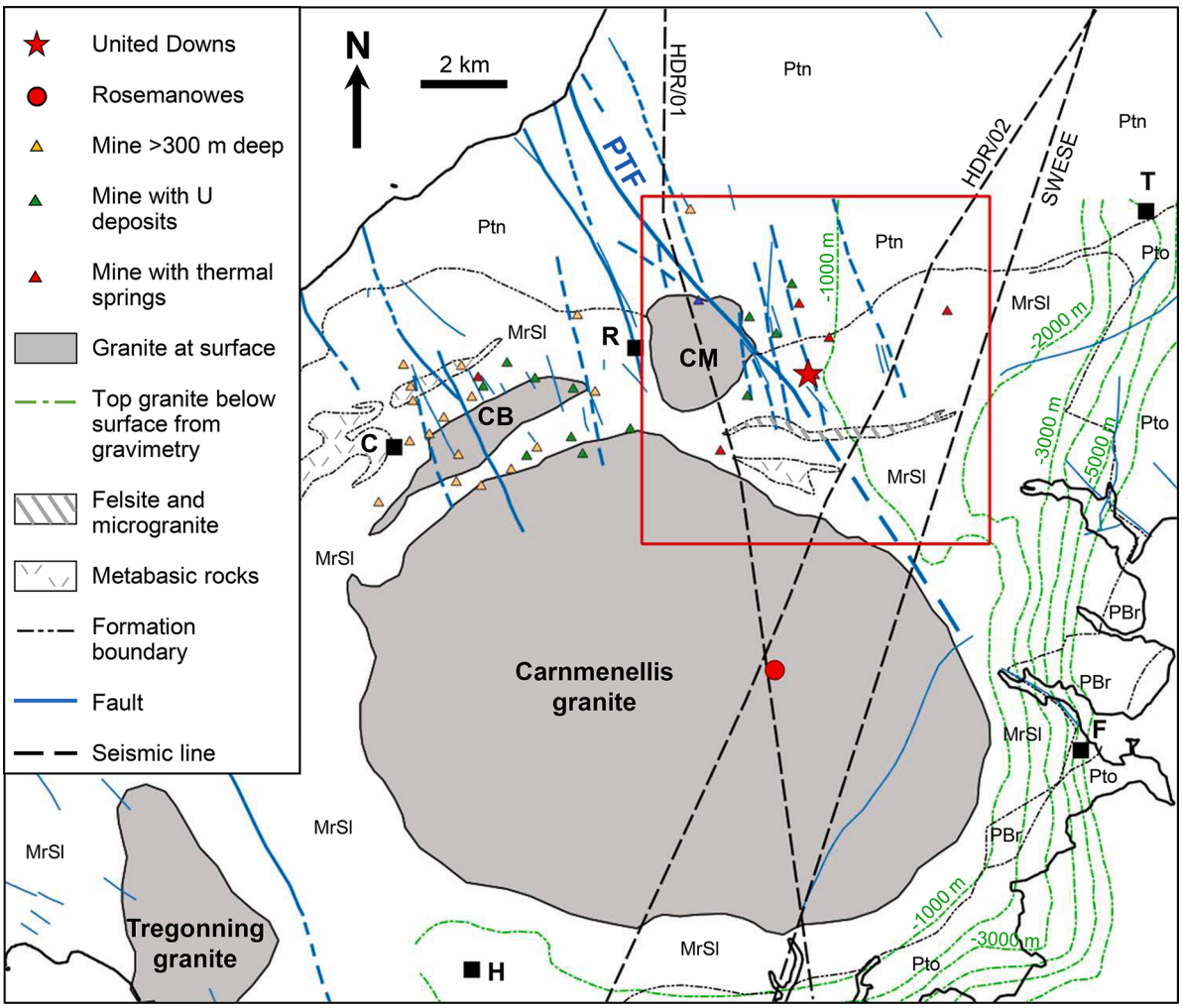

Fig. 2. Simplified geologic map of the wider project area. Graphical summary of information from different sources are displayed (redrawn after GeoScience Ltd. 2009). Isolines of top granite not displayed on the western and northern side of the Carnmenellis granite. The red square indicates the UDDGP model outline. Ptn: Porthtowan Formation, MrSl: Mylor Slate Formation, PBr: Porthleven Breccia Member, Pto: Portscatho Formation, all Devonian in age. Towns: T: Truro, F: Falmouth, R: Redruth, C: Camborne, H: Helston. (For interpretation of the references to colour in this figure legend, the reader is referred to the web version of this article.)

tens of metres to over 100 m (LeBoutillier, 2002). A conjugate set of NNE-SSE sinistral wrench faults is also locally present, but in subordinate numbers.

The Porthtowan Fault zone (PTF) belongs to this family of cross-courses and similar NW-SE striking structures that transect SW England (BGS, 1975). They are interpreted as strike-slip fault zones which accommodated periods of extensional (Devonian, Permo-Trias) and compressional (Variscan, Alpine) tectonics with periods of both dextral and sinistral movements. The PTF, as defined in the context of UDDGP, is composed of multiple converging faults that penetrate both killas and granite, resulting in this subvertical, NW-SE trending composite structure. Tentative evidence at outcrop of foliated and mylonitic granites suggest that the PTF may have been active during granite emplacement (GeoScience Ltd., 2009). In addition, Tertiary activity is possible by analogy with the Sticklepath Fault in Devon where several kilometres of Tertiary displacement, of variable sense, are recorded (Holloway and Chadwick, 1986).

3. Exploration and target definition prior drilling

A combination of factors influences the decision of any developer when selecting a potential site for geothermal development: geology, logistics, grid connectivity and community acceptance. The geology was based on a feasibility study to identify potential sites for a new deep geothermal drilling project in Cornwall (GeoScience Ltd., 2009). The site selection philosophy and process were strongly guided by experiences and results gained in the original 'Hot Dry Rock' (HDR) geothermal project at Rosemanowes where three wells were drilled to depths between 2,120 m and 2,650 m TVD in the Carnmenellis granite (Parker, 1989), some 6 km south of United Downs. The HDR site was chosen in part because the geology was expected to be relatively straightforward, comprising 'homogeneous' granite unaffected by significant faults.

As well as granite and fluid compositions, logging, testing and stimulation of the Rosemanowes HDR wells provided valuable information about the relationships between the fracture system, the in-situ stress field, and flow properties in the fractured granite. One of the key findings was the observation of micro-seismicity patterns during injection testing that indicated anisotropic fracture-controlled flow closely related to the NW-SE orientation of the maximum horizontal stress (S_H), as well as downward fluid migration (Pine and Batchelor, 1984). It was interpreted, that fractures favourably oriented to S_{Hmax} to be activated in shear or in transtension were preferential flow paths due to the impact of the anisotropic stress field on fracture apertures.

Therefore, the geological selection focussed on locations at or close to larger-scale faults oriented approximately NW-SE, close to S_{Hmax} on the assumption that they would potentially offer enhanced fracture permeability. This relationship was also implied by observations of hot

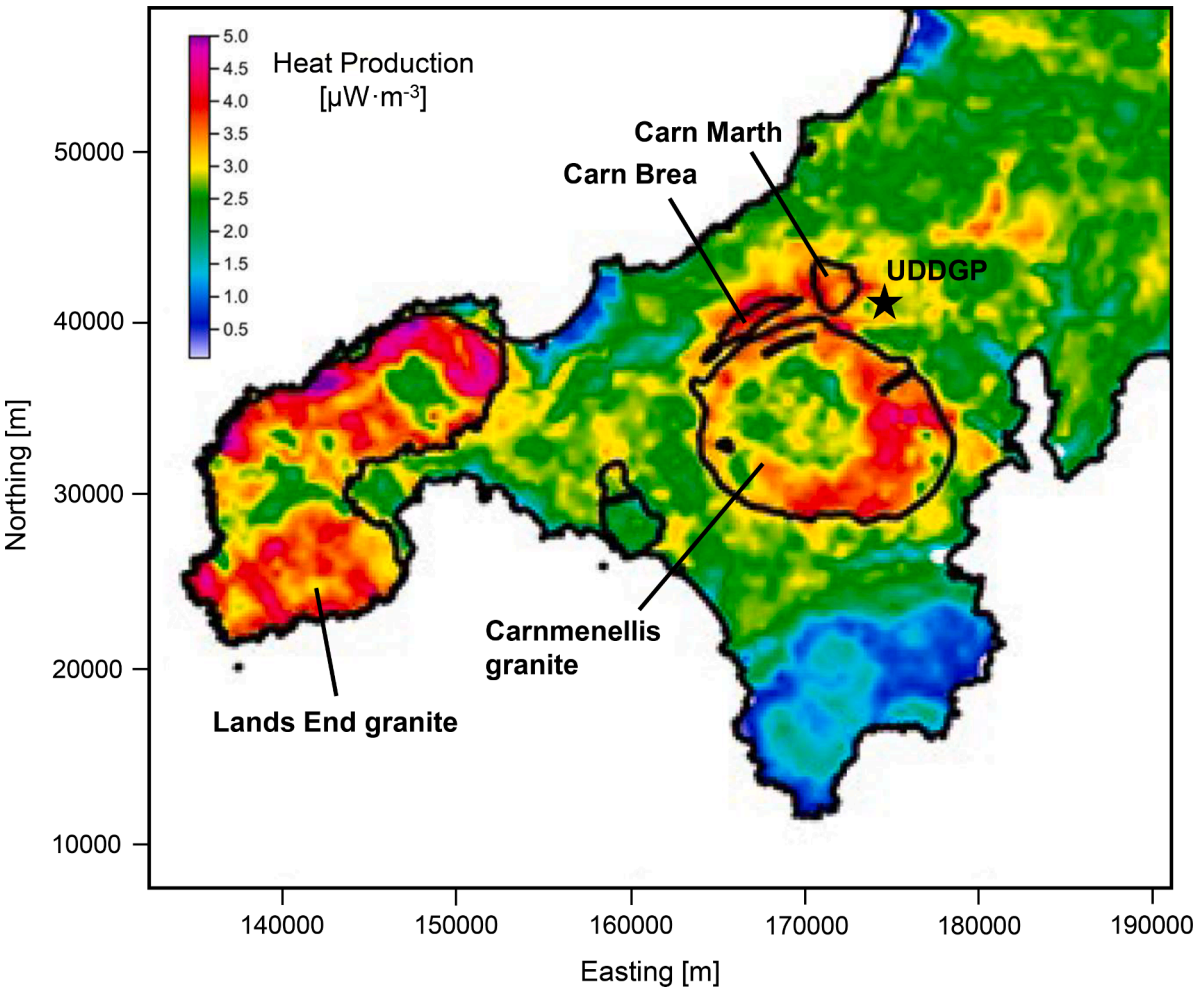

Fig. 3. Heat production map of south Cornwall (redrawn after Beamish and Busby 2016).

springs in mines and by occurrences of residual hydrocarbon (Baba et al., 2018), both of which tend to cluster around NW-SE faults and imply fracture permeability on geological timescales.

3.1. Evidence from mining records and outcrop

Geophysical surveys and other research had been performed by the British Geological Survey (BGS) and UK universities in the past. Some of which provided additional information about the site:

3.2. Gravity surveys

Gravity models have been used to predict the sub-surface shape of the Carnmenellis granite, including depth to top and to base of the granite body. Bouguer gravity surveys were performed in the 1950s and 1980s to infer the size and shape of the entire Cornubian batholith and its possible relations with major crustal structures (Willis-Richards and Jackson, 1989; Willis-Richards, 1990; Taylor, 2007). Estimates of batholith thickness are dependent upon assumptions about the geometry and depth of the intrusion, the mean density contrast with the host rock and the regional background Bouguer anomaly.

Modelling results and interpretations by Willis-Richards (1990) predicted a classical diapiric shape of the pluton with the base of the granite possibly honouring a mid-crustal gently south dipping reflector identified at c. 10 km depth in seismic profiles. This reflector (R2, see discussion below) was assumed to represent a north directed Variscan thrust. However, a shallower reflector was also identified at c. 8 km as discussed below. Most importantly for the project, the model predicts a steep granite/killas contact on the south and east side of the pluton along the line of the PTF, and a shallow (c. 1 to 2 km) table-like granite-top geometry to the northeast of the outcropping Carnmenellis granite in the UDGPP area.

An alternative gravity interpretation was given by Taylor (2007) who modelled the short wavelength, near surface gravity anomaly separately from a longer wavelength deeper anomaly. He constrained the model using the surface outcrop and near surface shape of the granite and considered more recent knowledge on magma ascent, intrusion mechanics and pluton geometries from various scales and outcrop analogues. His modelling suggested a tabular shape of the Carnmenellis pluton with a centrally located feeder and an estimated average thickness in the order of 3.7 km (with a range of 5.6 to 2.7 km for varying density contrasts) for the tabular part of the gravity model, consistent with estimates derived from empirical relationships for plutons.

However, thin granite cannot fully account for the observed heat flow at Carnmenellis, which calls for deeper layers of granite. Therefore, at pre-drill stage the Willis-Richard model was more favoured to predict the lithology at the target 5 km depth although the Taylor model, which raised the possibility of interleaved granite and Devonian sediments at the UDGGP site, could not be ruled out (GeoScience Ltd., 2009).

3.3. Seismic surveys

Seismic refraction profiles were acquired in the 1980's across Devon

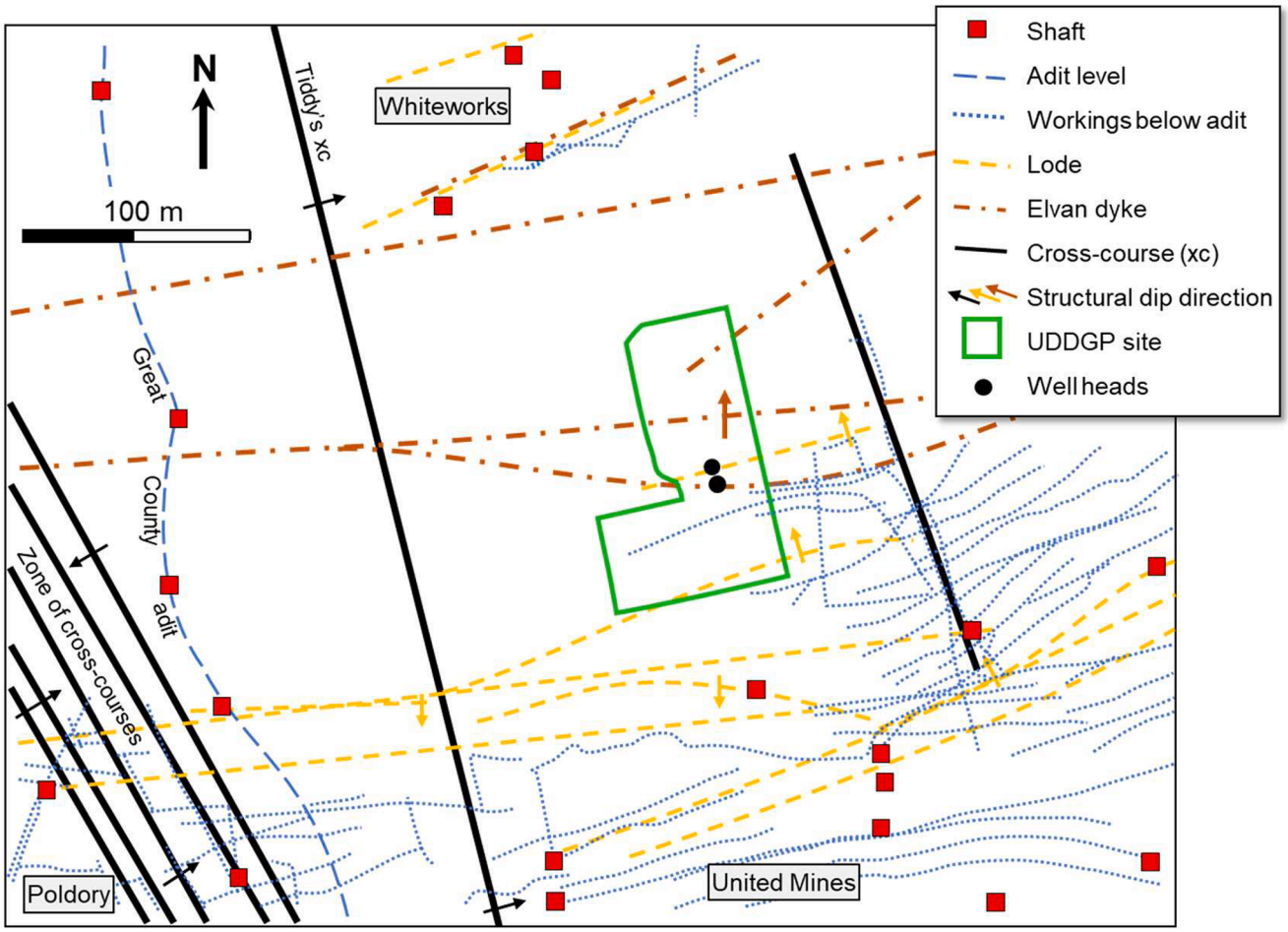

Fig. 4. Map of the drill site of UDDGP at the United Downs industrial estate east of Redruth with geologic features and known structures from mining activity. The PTF envelope as defined at surface is approx. 500 m to the SW of the drill site, just outside of the figure to the lower left.

and Cornwall (line SWESE in Fig. 2; Brooks, 1984), as well as two seismic reflection profiles across Cornwall as part of the Rosemanowes project (lines HDR/01 and HDR/02 in Fig. 2; Jones, 1991). The latter intersect close to the Rosemanowes site as shown on Fig. 2. On seismic, the granite is generally transparent, while within the killas some short reflectors are present, but the killas/granite interface itself could not be imaged. Three crustal reflectors (R1, R2 and R3) are recognized at depths greater c. 8 km. The shallowest reflector R1 seems to be close to the gravity-modelled base of the Carnmenellis granite (after Willis-Richards, 1990) and was interpreted either as a zone of high xenolith density, a Variscan thrust plane or the boundary of a separate intrusive unit in the granite. Interestingly an offset of the R2 reflector is observed in two seismic lines along the NE side of the granite, which can be tentatively correlated to NW-SE striking structures at surface. This could suggest that a significant NW-SE striking deep reaching structural zone (possibly a fault) exists at the NE flank of the Carnmenellis granite (Fig. 2). However, there is no clear evidence from the seismic reflection survey of structures within the granite at the UDGPP location nor of the exact location of the interpreted fault zone, due to poor resolution. Any correlation with the PTF is tentative.

3.4. Radiometric (gamma-ray) survey

Beamish and Busby (2016) revisited heat production values obtained as part of the original Camborne School of Mines HDR programme. These data were largely obtained at depths of less than 100 m and therefore represent shallow bedrock estimates and are subject to a high degree of vertical variability. This dataset was complemented with radiometric data from modern high-resolution airborne gamma-ray measurements (as part of the 2013 TellusSW survey). From spectral gamma-ray data, concentrations of potassium (^{40}K), equivalent thorium (^{232}Th) and equivalent uranium (^{238}U) in the rock mass are derived. The near-surface airborne estimates are adjusted to be consistent with the deeper borehole estimates. Corrected airborne estimates are then used to evaluate heat production across the survey area (Fig. 3).

Based on this data a temperature of 200 °C at 5 km depth in the Carnmenellis pluton is predicted (Beamish and Busby, 2016).

The records from mining activity in the United Downs area, although >100 years old and only covering the top 400 m of the 5 km deep drilling prognosis, provided important data on fault dip, dip direction, displacement, infill, and thickness (LeBoutillier, 2002; and references therein). This, together with the surface geological maps, was used to develop the conceptual fault model and prepare the drilling prognosis.

Mineral distributions in and around the Carnmenellis granite, which are manifested in lodes, elvans, cross-courses and uranium concentrations, give indications of paleo-fluid flow in general and locations where fluid flow was enhanced (GeoScience Ltd., 2009). Enhanced paleo-fluid flow is observed at the northern side of the Carnmenellis granite where a concentration of lodes is associated with the crest of a regional scale ENE-WSW striking anticline (BGS, 1975). Here, present-day hot springs in mines cluster at structural intersections of cross-courses with lodes (GeoScience Ltd., 2009). At the southern side of the pluton, mineralisation appears to be much less favoured, which implies less paleo-fluid flow in the subsurface.

Additional to geophysical surveys and mining reports, data collection and examination of key surface outcrops have been undertaken in

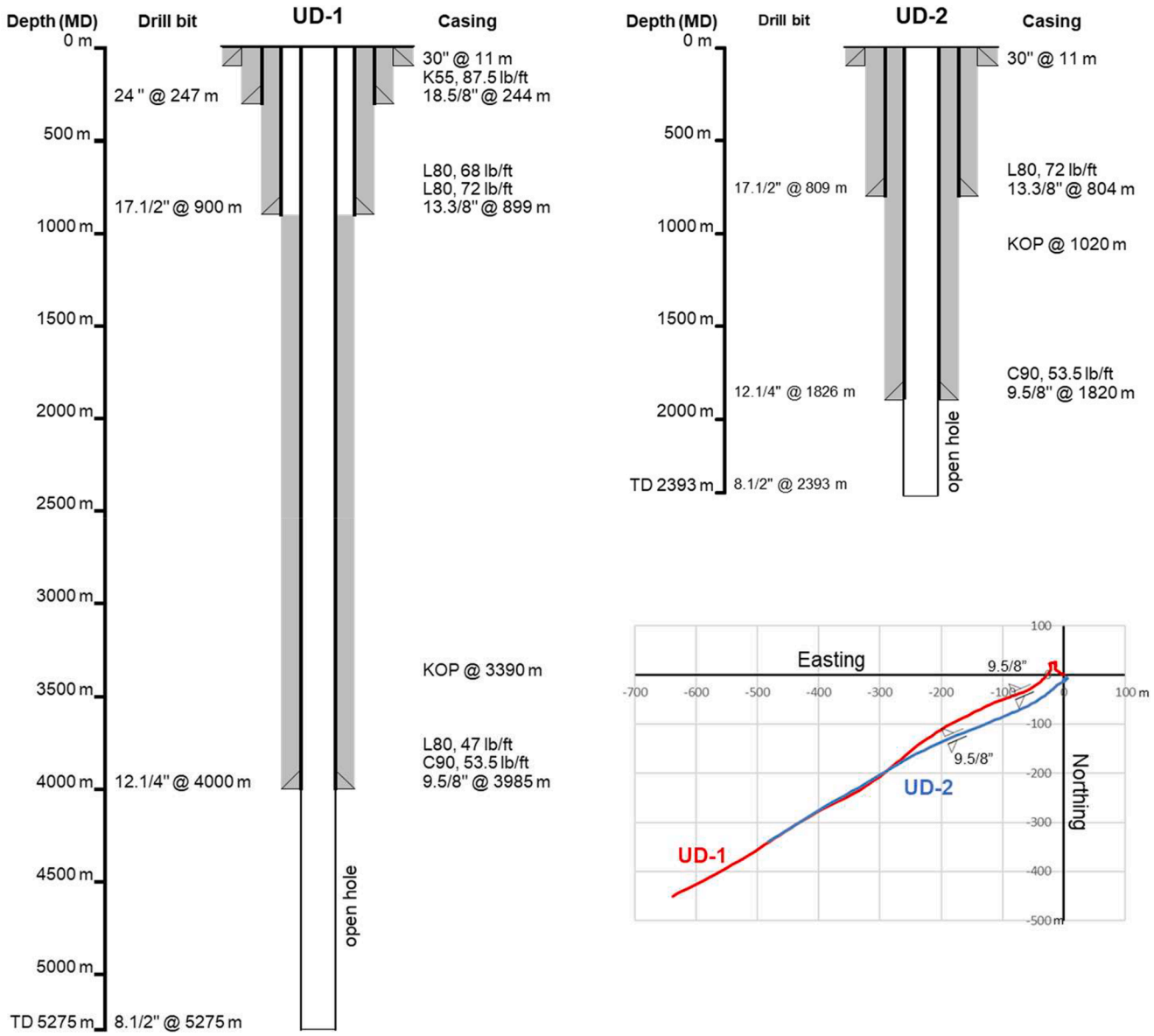

Fig. 5. Sketch of well completions and well trajectories in map view (scale in meters from wellhead) of UD-1 and UD-2. KOP: kick-off point, where drilling direction started to be deviated from vertical.

the region (GeoScience Ltd., 2009; Cotton, 2016). Only outcrops considered reasonably representative of lithology and especially structures belonging to the cross-course orientation at depth were taken into account.

3.5. Fault concept

As described above, SW England is cut by many NW-SE to N-S striking faults which are thought to have been episodically active during and since the late Carboniferous Variscan orogeny. These structures generally show strike-slip to oblique-strike slip displacements and, where exposed at surface or interpreted in mine data, are seen to have complex braided and segmented geometries in both vertical and plan view, with composite but generally moderately to steeply dipping/vertical fault strands.

Drilling target definition was therefore focused firstly on identifying the longer-length, larger displacement members of this fault group crossing the area because they are the most likely to be deeply penetrating. The second major criteria was that the selected structure should be situated in areas underlain by granite with high heat production such that the required bottom hole temperature could be accessed at shallower depth than otherwise. The distribution of hot springs in the mines, which indicate possible locations of deep-sourced groundwater flow, was also used to help select the target structure – the Porthtowan Fault zone.

Since there was no significant geophysical data with which to trace outcropping fault structures to depth, in order to make a drilling prognosis it was necessary to optimise the surface geology and mining related data and combine it with analogue structures (e.g. Kim et al., 2001; Holloway and Chadwick, 1986; Faulkner et al., 2008; Martel, 1990; Massart et al., 2010), seismic profiles (e.g. Lemiski and Brown, 1988; Bois et al., 1988), and with established structural geology models and concepts for major strike-slip fault zones.

Surface and mining data suggest that the PTF target structure is dipping steeply ENE, although there was no data to confirm this at depth. The PTF in detail was expected to be a broad zone (up to 400 m wide) at depth containing a number of discrete and complex fault planes with splay faults, some of which may strike at a low or even high angle to the main fault zone trend, and may have opposite dip directions (i.e. westerly). This implies that individual fault strands observed at or near

surface could not be realistically projected to kilometres depth. For drilling prognosis therefore, the PTF was envisaged as an 'envelope', defined at surface by two large boundary structures: the 'Great Eastern' and 'Great Western cross-courses'. The envelope was assumed to contain a highly fractured volume with increased structural permeability. The wells were also expected to encounter ENE-WSW striking mineral lodes and examples of the elvan dykes. Outcrop and mining data suggest that these structures, especially the mineral lodes, tend to terminate with depth and along strike. Therefore, their predicted intersections with the wells were considered uncertain at pre-drill stage.

4. Drill site selection and preparation

The specific drill site was determined by a combination of factors. The well was planned with a WSW deviation and a maximum inclination of around 35° at >4 km depth in order to make an orthogonal intersection with the target NNW-SSE striking, 80° ENE dipping PTF, and thus provide a good open hole intersection length through the structure. This required a site close to the PTF at surface but offset to the east. Other factors included the preference for brownfield sites, proximity to potential grid connections, suitable road access for large vehicles, and potential community acceptance.

A site was identified within an industrial estate on the old United Downs mining area, where, as shown in Fig. 4, a wealth of mining records was available to support shallow geological prognosis. These records also indicated the distinct possibility of drilling into old mine workings. Pilot holes c. 200 m deep were drilled close to the spud location to test for these workings, and the drilling programme itself made provision for such eventualities with initial casing run from surface to 900 m.

5. Drilling and logging UD-1 and UD-2

Two wells were completed between November 2018 and June 2019: The production well UD-1 reached a depth of 5,275 m MD (5,058 m TVD) and the injection well UD-2 a depth of 2,393 m MD (2,214 m TVD). Wellheads are 8 m apart.

The first well was originally designed to be the injector well to c. 2,500 m TVD. However, part way through the drilling it was decided to switch it to become the deeper production well owing to significant operational delays that had occurred. There were no major accidents or incidents and no lost time due to fishing.

Each well was drilled in Devonian metasedimentary rocks from surface but predominantly through granite (see Section 6) and were deviated to intersect the target fault structure to the west-south-west of the wellhead site. Both wells are completed as a barefoot well, with 8.5" open hole within the fault structure (Fig. 5).

The rate of penetration (ROP) while drilling was on average rather low in UD-1 and varied between 1 and 2.5 m/h in the 24" section, between 2 and 5.2 m/h in the 12.25" section, and between 2.5 and 6 m/h in the 8.5" section. Drilling breaks with ROP of usually around 10 m/h (up to 25 m/h maximum) were observed in zones of kaolinisation and/or intense fracturing or fault zones. These zones were generally identified in the cuttings (kaolinised or Fe-alteration) and some were associated with mud losses.

The drilling performance of UD-2 was similar but with less delays and non-productive time owing to the experience gained in UD-1.

Drill cuttings were generally sampled every 10 m, but this was reduced to 5 m in zones of particular interest. The cuttings underwent detailed description by the onsite geology team and subsequent mineralogical and geochemical laboratory analysis. Special emphasis was placed on identifying mineral species characteristic of lodes and cross-courses for correlation to other downhole data.

Standard wellsite mudlogging procedures were followed to collect data including MWD gamma ray, gas content and composition, mud losses and drilling parameters.

Mud losses occurred while drilling in both wells. As this was expected the mud weight was kept as low as possible (below 1.10 SG in the 24" and 17.5" sections and below 1.05 SG in the 12.25" and 8.5" sections) to reduce losses but still enable effective hole cleaning. Additionally, the mud flow circulation rate was reduced in the event of mud losses to decrease the mud losses. No further measures were taken to fight mud losses. However, mud losses decreased as drilling progressed. We assume fines migration into the loss zone to be the reason for this.

Wireline logging was performed in UD-1 comprising spectral gamma-ray (GR), 6-arm caliper, resistivity (STAR) and ultrasonic (UXPL) image (STAR and UXPL are brand names of Baker Hughes), cross multipole array sonic, laterolog, compensated neutron, and litho-density. Production logging (temperature, pressure, spinner) was also carried out. At a later stage during a workover phase in 2020, 19 sidewall cores were acquired below 4000 m in UD-1, their locations being carefully selected to be in or close to fractured intervals and especially those with evidence of permeability (e.g. mud loss locations, temperature log kicks). All these were used for characterising the reservoir and the granitic host rock.

Unfortunately, wireline logging has not yet been performed in UD-2 due to budget over-runs on UD-1.

6. Reservoir characterization

The characterisation of the encountered reservoir geology is based on drilling parameters, gas shows, mud losses, cuttings, and wireline logs (in particular the image logs) run in UD-1. The following main observations are made:

6.1. Lithology and fracture mineralisation

Three main lithologies were encountered by UD-1 and UD-2: metasedimentary rocks (killas), microgranite and granite. A description of each of these units, the depths they are encountered and a view of how they may fit within the regional context are outlined below:

6.1.1. Metasedimentary rocks

The upper 210 m of UD-1 is dominated by highly deformed, low-grade regionally metamorphosed and deformed mudstones of the Upper Devonian Mylor Slate Formation (Leveridge et al. 1990). This predominant fine-grained lithology also contains many quartz veins formed during Variscan low-grade regional metamorphism that pre-dates granite intrusion. The volume and scale (largely millimetric) of these quartz-rich structures influenced the ROP resulting in significantly lower rates than expected (c. 1-3 m/h).

QEMSCAN analyses carried out at the Camborne School of Mines, University of Exeter of the upper 210 m of UD-1 showed mineral assemblages akin to those encountered in the steeply dipping lode systems of the United Downs mining district. The results revealed a range of oxide-sulphide mineralisation, showcasing nearly every mineral to have been exploited in that area including occurrences of tin, copper, zinc, and wolfram.

6.1.2. Microgranite

At pre-drill stage the estimated depth to the granite top was c. 500 m (±200 m), based on old mining records (none of which encountered granite in the local area) and re-processed coarse resolution gravity data. However, both UD-1 and UD-2 penetrated heavily greisened and kaolinized fine grained 'microgranite' from 210 m MD to c. 740 m MD. Optical analysis of the cuttings showed a dominance of sub-rounded quartz fragments, with variable quantities of tourmaline (c. 5-15%). Much of the kaolinite was lost to the drill mud, and thus it was not possible to determine modal proportions. Although unexpected at the time, this lithology has since been identified as a NNW-dipping microgranite-rhyolite dyke, colloquially called 'elvan' in mining terminology, which does not reach ground level and had therefore not been

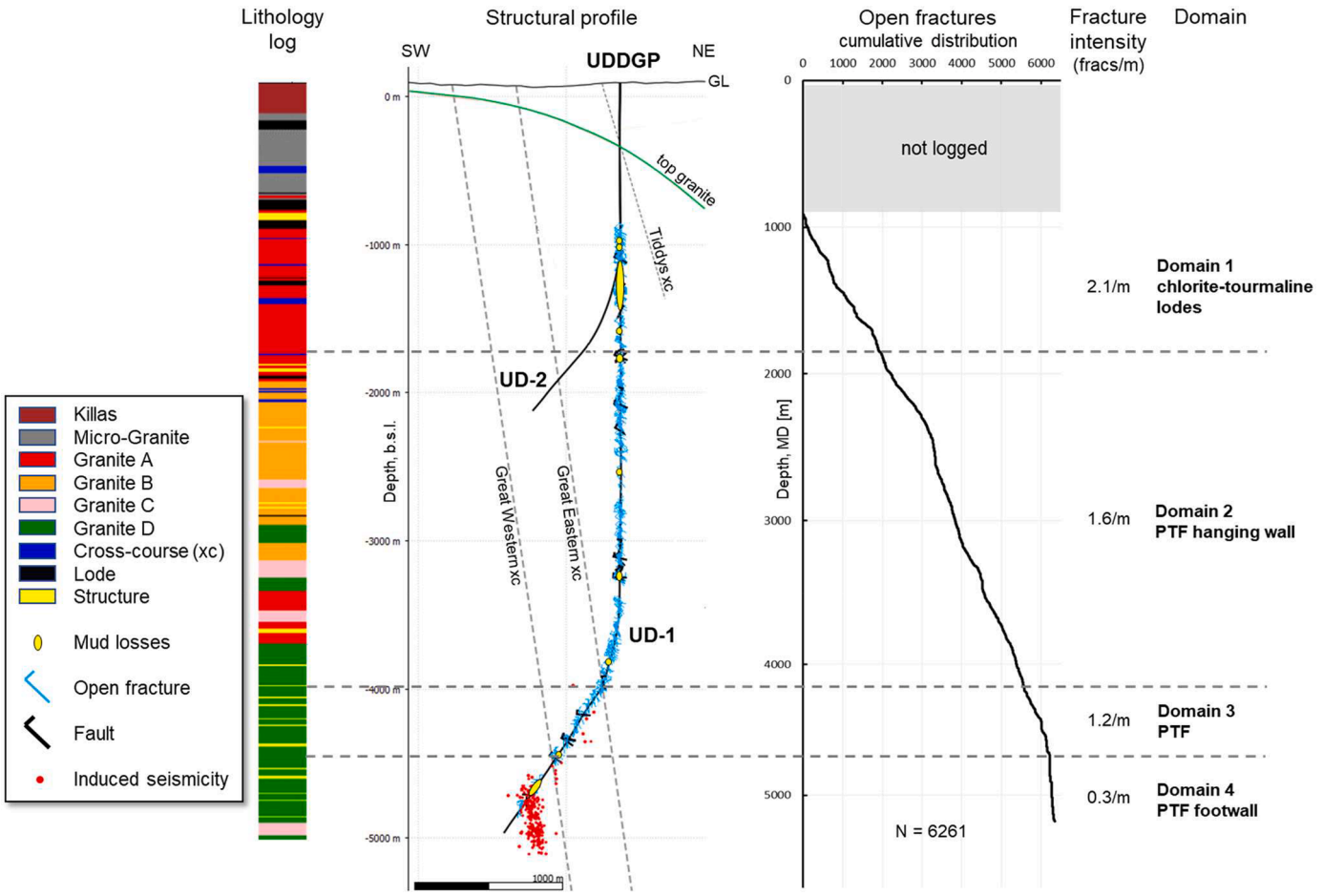

Fig. 6. Fracture data along UD-1 as interpreted from ultrasonic (UXPL) image logs. Note depth scale of the structural profile is true vertical depth below sea level. Cumulative fracture distribution and lithology log originally in measured depth below ground level are shifted and stretched to fit the true vertical depth scale.

previously mapped. Elvans are commonly referred to in mining records throughout Cornwall and are known to exhibit irregular geometry. The elvan drilled is thought to be steep to subvertical and its emplacement was probably controlled by interaction of ENE-WSW striking extensional faults with NNW-SSE striking strike-slip faults at the eastern margin of the PTF.

6.1.3. Granite

The lower c. 4.2 km of UD-1 is dominated by granite and is subdivided based on variations in cuttings texture, mineralogy, and gamma ray into four main types (Granites A, B, C and D). Optical analysis show variations in the proportions of darker minerals (tourmaline, biotite), and variable colours of mica that indicate subtle changes in the biotite mineral group. Step changes in the gamma ray values also define the granite types, which respond primarily to variations in the U and Th bearing accessory minerals. These mineralogical and gamma variations reflect the composite nature of the granite, which are a result of magmatic processes that occurred during the generation and emplacement of the granites.

The modal mineralogy of the granite determined by QEMSCAN on cuttings indicated that the lower 4 km of the hole was characterised by two mica (G1) and muscovite granite (G2) according to the Simons et al. (2016) classification scheme. Further, nearly all coarse cuttings below 740 m plotted within the monzogranite field on the QAP classification which is consistent with the granites encountered during the Hot Dry Rocks project at Rosemanowes.

6.2. Fracture network characteristic

Sources of fracture information are drilling data (cuttings analysis, ROP, mud losses and temperature) from both wells together with wireline images from UD-1. Both micro-resistivity (STAR) and ultrasonic (UXPL) images were acquired, the latter giving full wellbore coverage and hence providing the most comprehensive set of fracture data. Images were collected from the 12.25" and 8.5" sections of UD-1 from 906 to 5,206 m MD.

The fracture data characterised in the following are interpreted from ultrasonic (UXPL) image logs. The image covers the full borehole wall with a resolution of 256 data points per revolution (approx. 1.4° azimuth) and 5.08 mm depth increment with beam width of 8 mm at 250 Hz. Depth of investigation is zero (i.e. reflection on the borehole wall). The UXPL tool records time and amplitude of the returned signal. The representation in time displays the radius/shape of the borehole. We have mainly used the amplitude (i.e. reflectivity) representation of the ultrasonic image for fracture identification and characterisation.

The UXPL tool essentially only sees open fractures unless a closed fracture leaves an impression in the wellbore wall when drilled (such as a ridge) or there is a high contrast in reflectivity between mineralisation and host rock. Therefore closed / mineralised fractures will be almost invisible to the UXPL tool. However, open fractures are low amplitude features and higher confidence features are those in regions of good image quality, have wide traces and which typically transect the borehole. For completing the fracture data set the micro-resistivity (STAR) image needs to be interpreted and compared with the ultrasonic (UXPL) image interpretation. This work is pending. However, from the

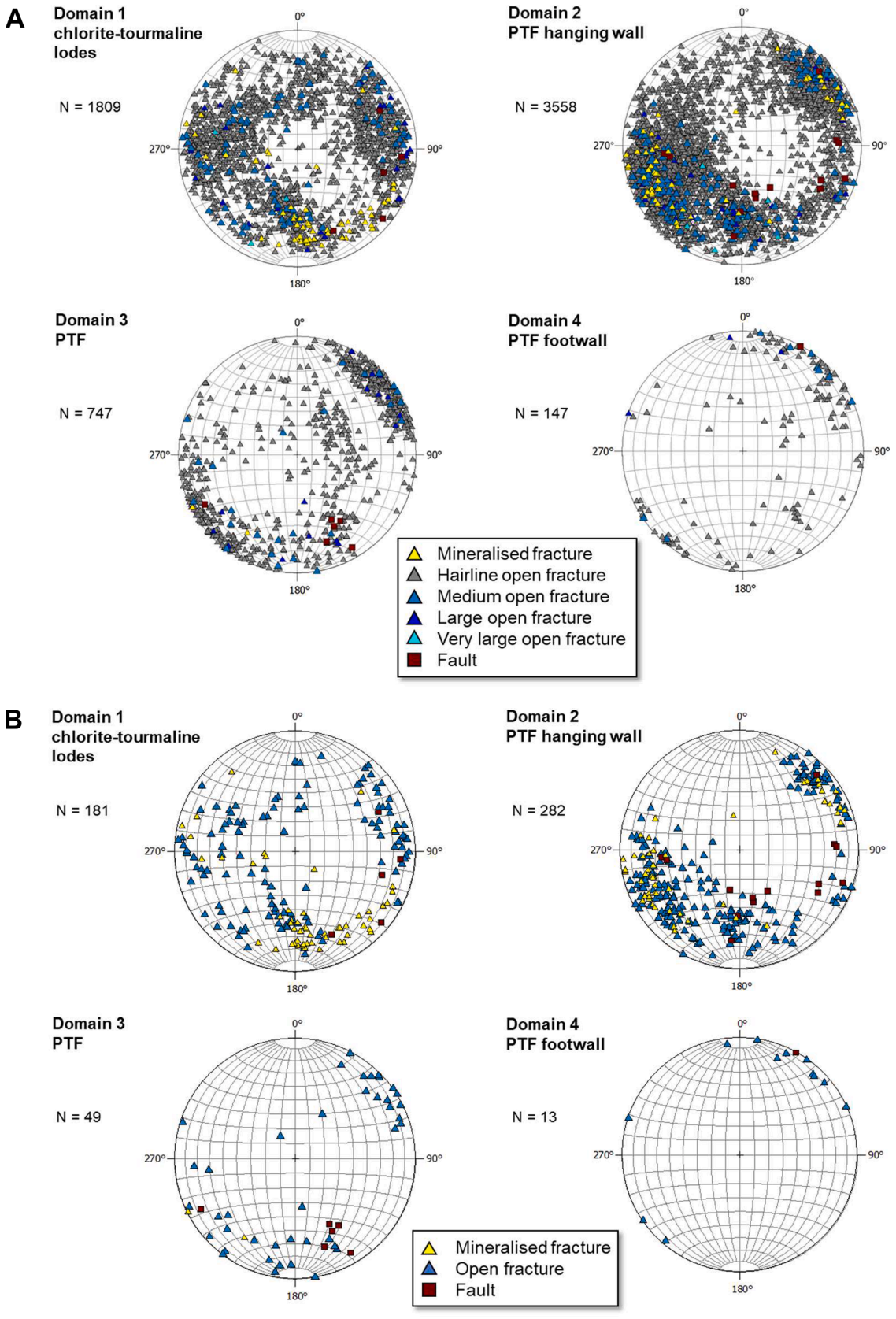

Fig. 7. A) Stereo plots of all fractures used for the cumulative fracture distribution plot in Fig. 6. The legend captures variation in apparent aperture of open fracture picks. B) Stereo plots of high confidence fracture data only, i.e. without 'hairline open fractures'. All stereo plots are in equal area projection, lower hemisphere. 'Mineralised fractures' refer to fractures filled with porous mineral aggregates such as micro crystalline tourmaline in the lodes, features in image with lower amplitude than granite but much higher amplitude than fracture porosity. The thick mineral fills in the lodes (multi meter apparent thickness in wellbore intersection) for example often have wonderful, banded textures and are clearly neither granite nor open.

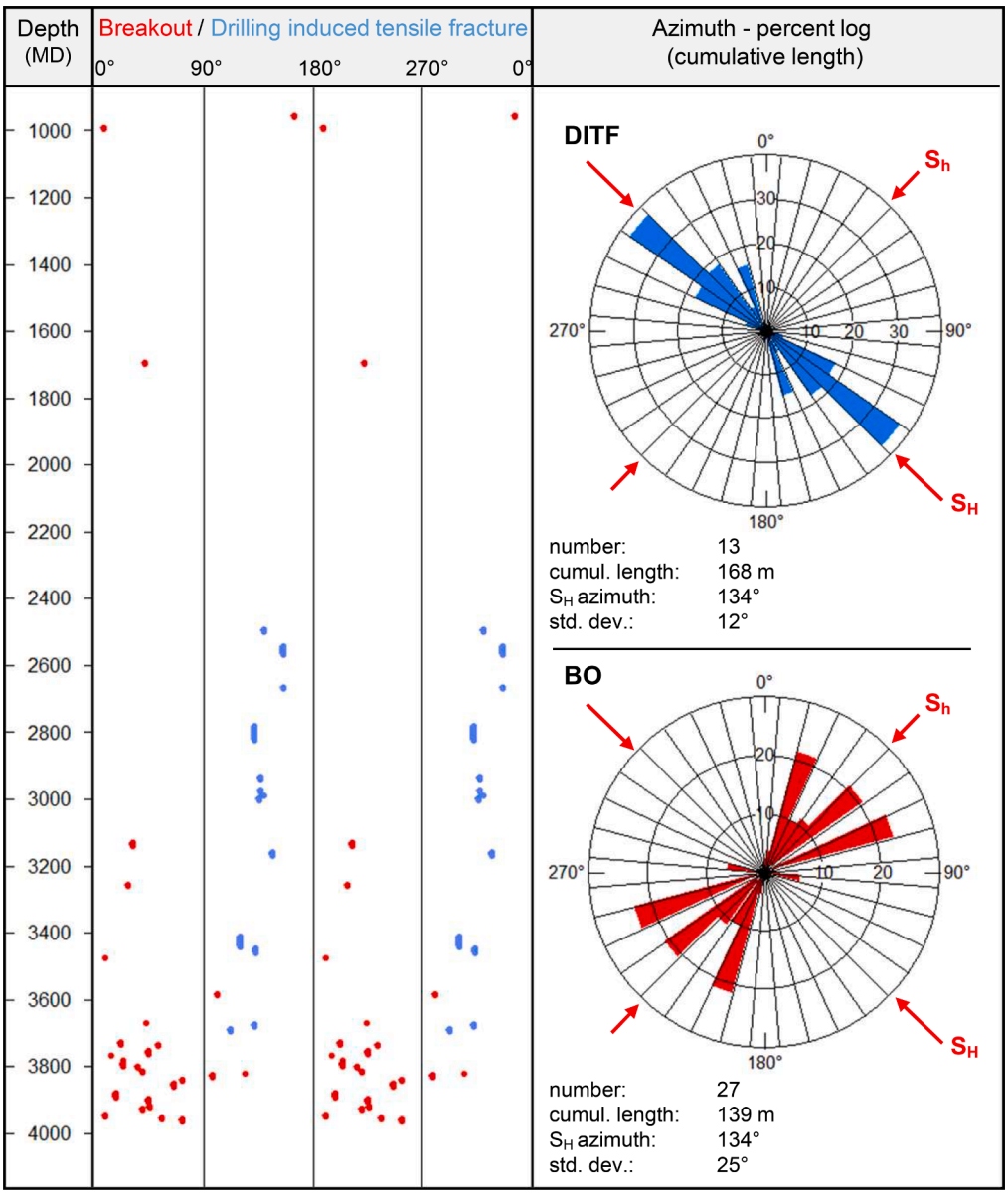

Fig. 8. Stress orientation derived from borehole breakouts (BO) and drilling induced tensile fractures (DITF) observed in the ultrasonic (UXPL) image log of the 12.25" section in UD-1. Note, that this section is nearly vertical. Maximum deviation from vertical is 15° in the lower 200 m, where the scatter in BO orientation is the highest. Mean orientation of maximum horizontal stress S_H is 134°.

geothermal point of view only open and partially open fractures are important as they contribute to fluid flow / heat exchange in the subsurface. Therefore, we regard the fracture interpretations from the UXPL image sufficient for reservoir characterisation, with the advantage of full borehole coverage in contrast to the 6-arm micro-resistivity image (STAR).

Two sets of fractures were identified: the major set broadly trending NW to NNW (cross-course) and the minor trending ENE (sub parallel to lodes). Mineralised and open fractures were distinguished, and the evidence suggests potential fracture porosity resides primarily in the cross-course fracture set, whilst a subtle 20° to 30° anticlockwise rotation of the open fracture subsets occurs with depth. Fracture dips are conjugate and variable; the cross-course-parallel set is generally steep to sub-vertical (c. 30°-90°) and the lode-parallel set is more shallow dipping (c. 20°-70°).

The following summarises the distribution of the fracture intensity and orientation data with depth (Fig. 6):

There is a general decrease of fracture intensity with depth but with an abundant evidence of open fractures (i.e. low amplitude features in the ultrasonic image log) persisting. This may partly reflect a reduction in fracture aperture with increasing overburden, rendering it more difficult to resolve open fractures in image logs.

Four structural domains are defined based on changes in fracture intensity and orientation, as well as fracture types and fill character:

- Domain 1 is characterised by northerly dipping mineralised fractures (i.e. lodes) cut by both N-S (major) and ESE (minor) open fracture sets with uniformly high fracture intensity (mean 2.1/m) throughout.
- Domain 2 is characterised by a decrease in open fracture intensity with depth (mean 1.6/m), a decrease in mineralised fractures (lodes) with depth, more variable open fracture intensity probably due to faults intersecting the well, the persistence of the minor ESE set, but shows an anti-clockwise rotation in strike of the major NW to NNW set of 20°. Fractures predominantly dip NE.

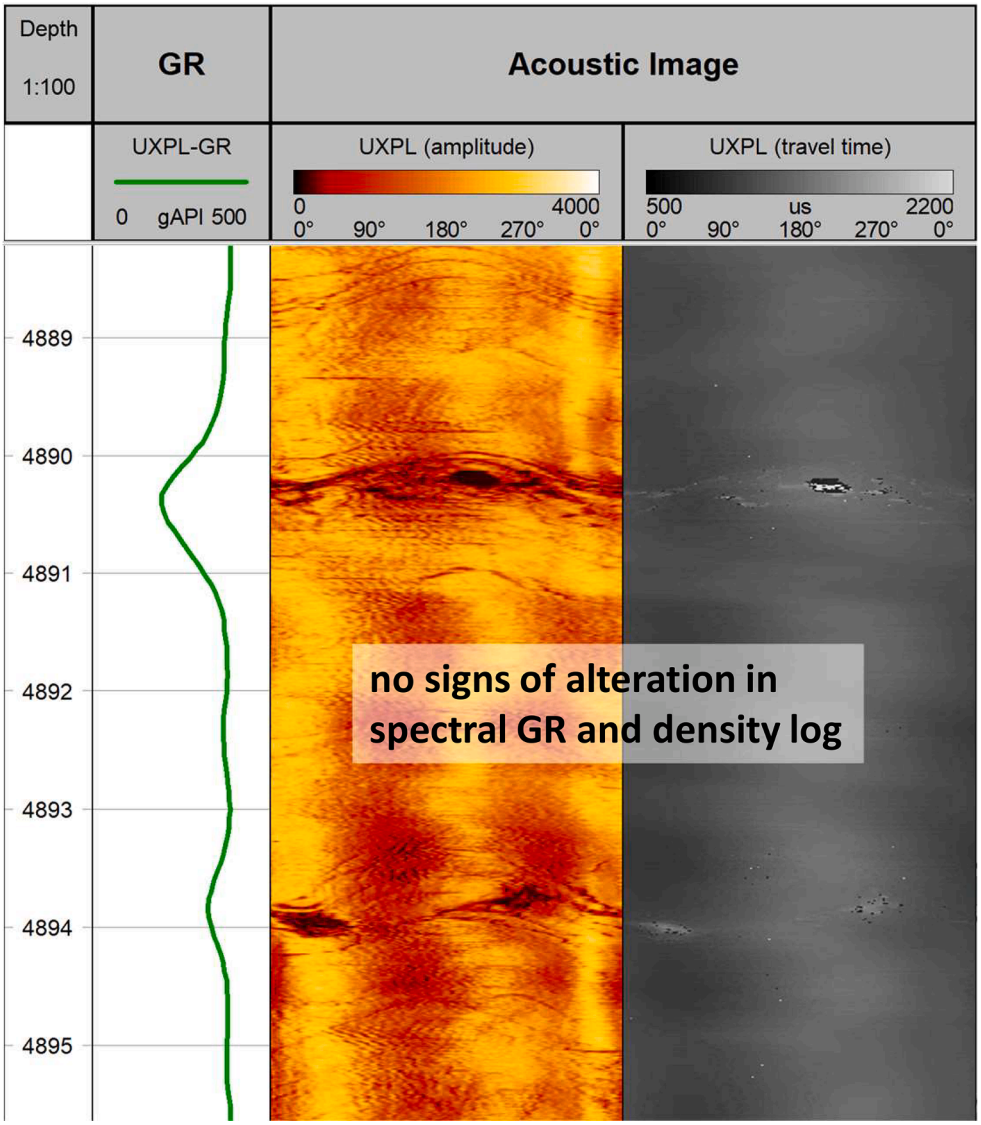

Fig. 9. Open fractures at 4,890 m MD in UD-1. This feature correlates with sudden high ROP and high mud losses during drilling, a negative gamma-ray peak and a significant change in temperature gradient (Fig. 10).

- Domain 3 is interpreted as a zone of brittle fracturing (mean open fracture intensity 1.2/m) superimposed on the eastern or hanging-wall side of what may be a pre-cursor ductile PTF structure represented by what could be a mylonitic fabric visible in the image. Alternatively, the fabric could be geomechanically induced in the prevailing stress environment below 4 km. Fractures are clustered and there is a further anticlockwise rotation in strike of both open fracture sets to NW (major) and ENE (minor) (Fig. 7), and clear evidence of a fractured volume from the drilling parameters, gases, and possibly the reduction in cuttings size below c. 4,300 m MD (although this may be due to a reduction in the capability of the mud flush to lift cuttings to surface).
- Domain 4, where a marked reduction in open fracture intensity (mean 0.3/m) is observed while the (possible) mylonitic fabric persists, is interpreted as the PTF footwall. Open fractures are clustered and the anticlockwise rotation in strike is more marked than in domain 3. A significant mud loss zone occurs within it and fractures may preferentially dip SW rather than NE. Also, micro-seismicity was recorded here during both drilling of the section and subsequent hydraulic testing (Fig. 6).

The overall structural configuration is considered to be the product of episodic reactivation phases (Permian to Tertiary) of linked fault systems striking mainly NNW-SSE (i.e. PTF or 'cross-course' trend) and ENE-WSW (i.e. 'lode' trend). These structures have both extensional and oblique strike-slip components, the net effect being high levels of fracturing and associated (mainly early Permian to Triassic) mineralisation, at least at higher levels.

Figs. 6 and 7 display the structural data interpreted from ultrasonic (UXPL) image logs in UD-1. Structural complexity is generally high. However, due to the scanline data sampling along the wellbore trajectory, the spatial correlation to observations at surface or in mines remains uncertain due to the large distance and absence of clear reference structures/horizons. The fracture statistics along the open hole section between 4,000 and 5,200 m MD suggest that the PTF envelope is encountered between 4,100 and 4,700 m MD. However, mud losses while drilling and induced seismicity (as described in the following section) indicate a hydraulically active structure or structures at greater depth (at 4,890 m MD). This mismatch in observations means that the definition (structural vs. hydraulic) of the PTF at reservoir depth is unresolved, although this is not unusual in fractured formations due to the heterogeneous distribution of flow.

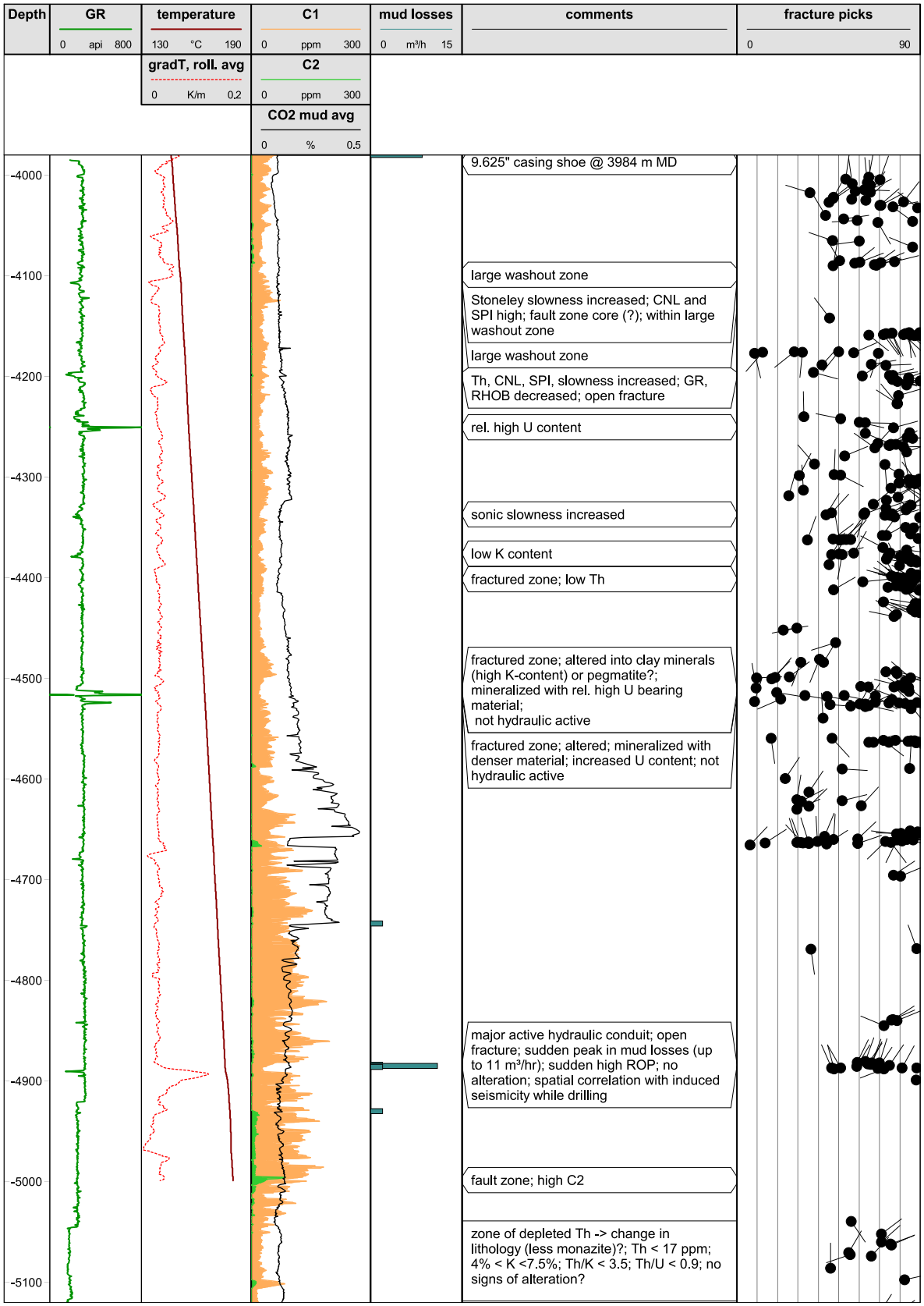

Fig. 10. Reservoir section of UD-1. Depth scale in measured depth. Logs from left to right: gamma-ray, temperature/temperature gradient (rolling average), gas shows (C1, C2, CO2), mud losses, comments from other log analysis (spectral gamma-ray, caliper, density, sonic), fractures picked on ultrasonic image.

6.3. Stress

Stress induced features (i.e. borehole breakouts, BO, and drilling induced tensile fractures, DITF) are interpreted on ultrasonic (UXPL) image logs from the 12.25" and 8.5" sections. Breakouts are locally developed in the 12.25" section, notably in the lower part (Fig. 8), and extensively in the 8.5" section. The high scatter in BO orientation below c. 3,600 m MD may reflect the increasing borehole inclination (from near vertical in the upper part to up to 15° in the lowest part of the 12.25" section) and influence of active fault structures. The breakouts are narrow and deep indicating high horizontal stress anisotropy. In a first attempt we have used orientations of BO and DITF from the 12.25" section only to infer statistically the mean maximum horizontal stress S_H (Fig. 8). The borehole inclination of the 8.5" section is greater 15° and therefore regarded more problematic.

In total 27 BO with a total length of 139 m are picked between c. 900 and c. 4,000 m MD. The derived S_H azimuth is 134°±25°. Within the same interval 13 DITF with a total length of 168 m are picked between c. 2,500 and 3,700 m MD. The derived S_H azimuth is 134°±12° (Fig. 8). The coincidence serves to provide high confidence in the derived stress orientation. Also, this value is in accord with observations at Rosemanowes and South Crofty Mine from overcoring, hydrofracturing, and focal mechanisms (Pine et al., 1983a, 1983b; Batchelor and Pine, 1986).

The vertical stress S_V was calculated from wireline density logs. There were subtle variations in the density log and the best fit equation for the S_V gradient is:

$$S_V\ grad = 25.275\ MPa/km$$

The pore pressure gradient with depth is 9.494 MPa/km below static fluid level at approx. 61 m below ground level.

The minimum horizontal stress S_h magnitude has been adapted from the hydrofracturing tests made at Rosemanowes (Pine et al., 1983b). Refracture pressures were taken to represent the re-opening of the fracture created during the first cycle and subsequently a good approximation to the minimum horizontal stress. Fitting a linear trend through these refracture pressures with vertical depth gave the following estimate of the minimum horizontal stress:

$$S_h\ grad = 13.21\ MPa/km + 3\ MPa$$

The uncertainty lies in not knowing if the fractures are true Mode I re-openings (tensile) of fractures or if there is some shear component included, Mode II or III.

The maximum horizontal stress S_H magnitude estimation relies on micro-seismic observations as an indication of the stress anisotropy at depth and was adapted from Rosemanowes. With an estimate of the S_h magnitude, the formation pressure and the fracture fluid pressure required to initiate slip along a fracture of known orientation then the magnitude of the maximum horizontal stress magnitude was deduced using an assumed coefficient of friction μ of 0.8:

$$S_H\ grad = 25.99\ MPa/km + 5.9\ MPa$$

The stress regime is strike-slip and critically stressed for shearing on appropriately oriented fractures. The orientation of the fractures within the in-situ stress field favour enhanced fracture permeability due to elevated dilation and slip tendency. However, the mud losses while drilling and the induced seismicity at depth show that the conditions do look favourable for persistent open fractures at depth.

A more detailed study on the stress state incorporating the observed induced seismicity at United Downs is ongoing and will be the subject of a subsequent paper.

6.4. Indications for hydraulic active zones

Hydraulically active (i.e. conductive) zones were recognised during drilling and identified from wireline logs. In UD-1, mud losses during drilling were minor except in specific short intervals associated with structures intersecting the wells. Those of most interest to the project objectives were dynamic losses of up to 11 m^3/h, which occurred in the 8.5" section of UD-1 below 4,000 m, especially across the interval 4,850 to 5,080 m MD which coincided with sudden high ROP while drilling, a clearly visible open fracture zone in the image logs at 4,890 m MD (Fig. 9), and a distinct anomaly in the temperature gradient (Fig. 10), measured under thermally equilibrated conditions in the borehole after a longer period of nonoperation. These are taken as firm indicators of natural permeability.

Other anomalies in temperature gradient were observed, for example at 4,250 m MD, often correlating with pronounced GR peaks indicating a high content of mobilized uranium within a fracture zone (Fig. 10). However, these were not necessarily associated with mud losses.

In UD-2 dynamic mud losses started at 2,374 m MD with 4.5 m^3/h and increased to 10 m^3/h by 2,377 m MD. This zone is correlated to the eastern edge of the PTF. After reaching final depth static losses were observed to be 2 m^3/h.

6.5. Induced seismicity

While drilling the reservoir section of UD-1 in total 18 seismic events with magnitudes ranging between ML -2.07 and -0.38 were detected and localised using relative hypocentre location techniques with the largest event as the master event (Rothert, 2019). All seismic events are close to the well and correlate with the depth of drill bit at the time of occurrence. Therefore, all events are regarded as induced seismicity.

Two seismic clusters could be identified (Fig. 6): The upper cluster of 6 events occurred as the drilling assembly was being run-out-of-hole from 4,417 m MD. The hypocentres of the events are not well defined. Within their uncertainties, they can be associated with a positive gamma-ray peak at 4,253 m MD indicating a fault zone with relatively high U content (precipitation from mobilised uranium?). The events of the lower cluster (12 events) correlate in time and space with the mud losses at 4,890 m MD. Therefore, it might be suggested that the seismic events were caused by fluid overpressure.

During injection testing of UD-1 in August and September 2020 roughly 250 induced seismic events were detected of up to ML 1.7. The majority of these events correlate with the lower seismic cluster already identified during drilling.

Major observations of the developing induced seismicity are:

- The trends appear to be close to that of the open fracture subsets in domains 3 and 4 (Section 6.2), as discussed below in Section 8.
- Most events occur close to the mud loss zone during drilling (@ 4,890 m MD).
- The vertical reservoir growth is progressive over time and predominantly towards greater depths.
- The seismicity volume (i.e. the volume of the seismic cloud) tends to extend throughout the injection tests.
- Maximum event magnitude appears to increase with depth.

Induced seismicity was regarded as a potential issue from the very beginning. A seismicity prognosis was therefore developed prior to drilling UD-1 (Carstens and Wittmann, 2019a) and updated after completion of UD-1 (Carstens and Wittmann, 2019b) to consider the new subsurface information and the observed induced seismicity while drilling the reservoir section of UD-1. In fact, the first prognosis suggested stress conditions at a depth level of 5 km and deeper to be extremely close to criticality so that minor stress perturbations could be sufficient to cause slippage on a pre-existing favourably oriented fault or fracture. Observation data from UD-1 (mainly structure and stress orientations) are within the range of parameter assumptions made in the first prognosis and the observed seismicity during drilling confirmed the near-critical stress state derived in the prognosis.

No induced seismicity has been observed while drilling and injection

Table 1
Data used to setup the structural reservoir model of UDDGP. bFN: background fracture network, fzFN: fault zone fracture network.

Data source	Input data in modelling	Data quality
Surface mapping	Fault traces at surface	medium
	Surface geology	high
Mapping in mines	Fault trend at depth down to approx. 400 m	medium
Observations in outcrops	Fracture network characteristics near surface (bFN, fzFN)	high
Rosemanowes HDR project	Fracture network characteristics at greater depth down to approx. -2.500 m (bFN)	high
Gravity modelling	Top granite at depth	medium
Well completion	Section of injection / production	high
Well data (cuttings)	Stratigraphy along well	high
Well data (image logs)	Pinpoint fault zone at depth	high
	Fracture network characteristics along well trajectory (bNF, fzFN)	high
Induced Seismicity	XYZ of hypocentres (seismic cloud of pressure response)	medium-high

testing UD-2 so far, despite relatively large volumes of fluid injection. A final injection run is planned for June 2021, during which time geofluid will be pumped from the deep well and injected into UD-2.

7. Well testing

Directly after completion of UD-1, a short air-lift production test was carried out on 2nd May 2019 with concurrent production logging. Emerging foam from the chimney of the degasser led to a premature termination of the test without reliable test results. The test was considered to be a write off and the rig was skidded to the second well to be drilled directly afterwards.

Two short injection tests were performed in UD-2 after completion. The first was performed with the drill string remaining in hole (BHA pulled into casing) and the second after the string was pulled out of hole. The first injection test was performed at 3 different flow rates ranging between 500 and 2000 l/min, and the second injection test at 3 different flow rates of between 900 and 4000 l/min. Total injected volumes of fresh water were 61.5 m^3 and 93.5 m^3 respectively. Maximum annulus pressure at the well head was 82 bar.

As the injection rates for UD-2 were already within the target range for the power plant operation, attention was focused on the stimulation of UD-1 to improve flow rates. These consisted of three phases:

- Phase 1 – Step-Rate Injection Testing (August 2020)
- Phase 2 – Extended Injection Testing (September/October 2020)
- Phase 3 – Low Pressure Extended Injection Testing (October 2020 – February 2021)

The results of this process and the associated induced seismicity will be the subject of a separate paper. Overall, there was a substantial improvement in injectivity from the start of Phase 1 to the end of Phase 3.

8. Reservoir modelling

The structural reservoir model incorporates relevant horizons, faults, fracture networks and well trajectories. Input data are derived from surface mapping, mapping in nearby mines, observations in outcrops and from the Rosemanowes HDR project (fracture network

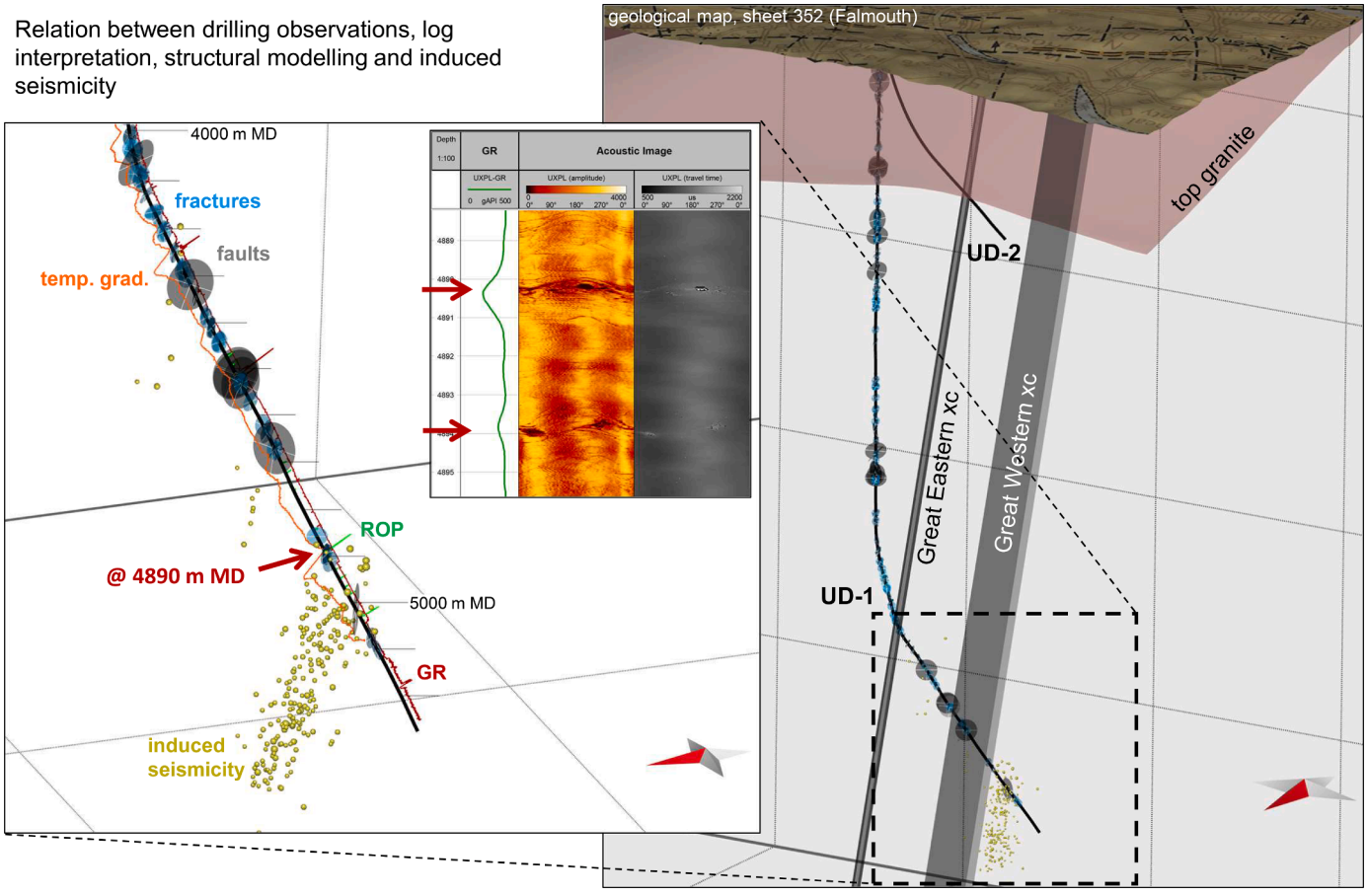

Fig. 11. Scene from the structural reservoir model with the open hole section of UD-1 highlighted. View direction is from the northwest. The image log in the inserted figure is essentially the same as in Fig. 9 displaying the main mud loss zone during drilling.

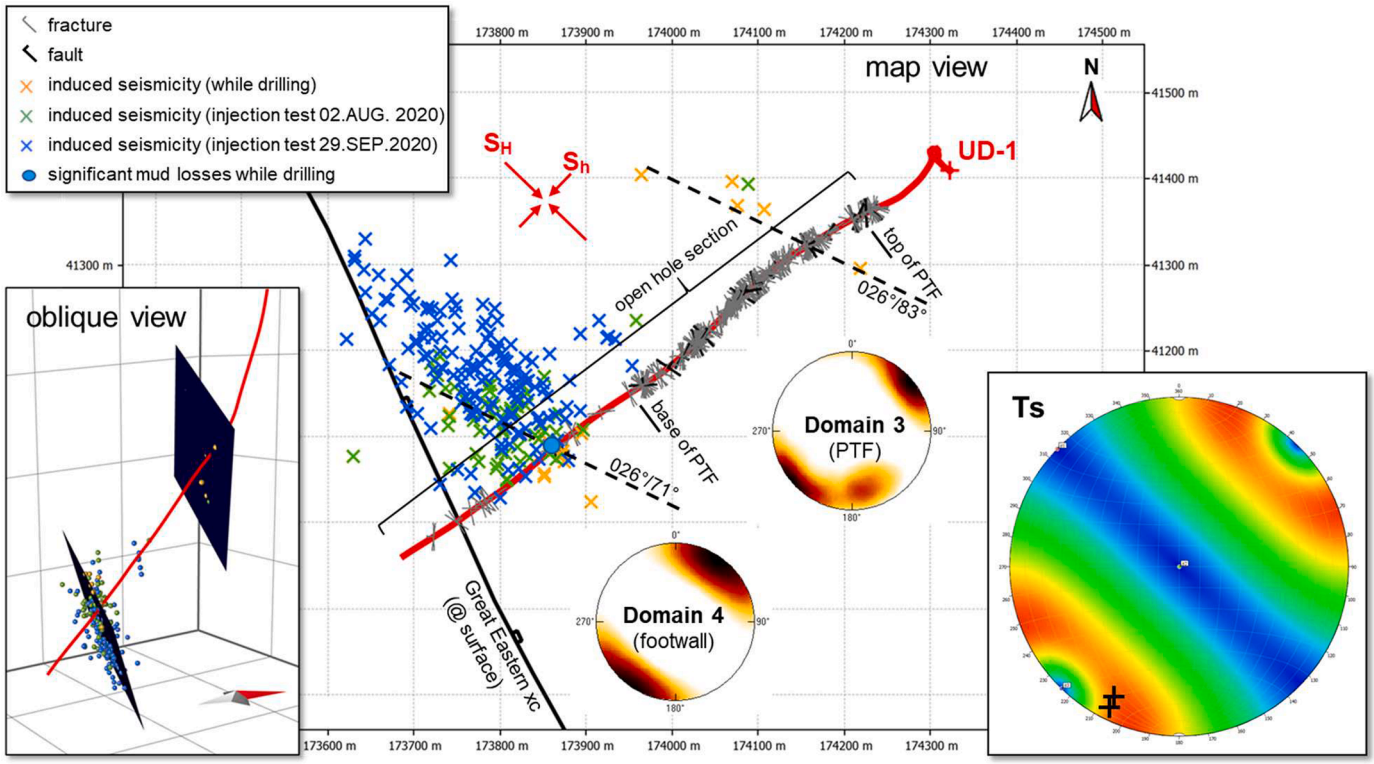

Fig. 12. Map view of the reservoir section along UD-1. Polar plots (lower hemisphere) of fracture poles of domain 3 and 4 display density contours. The two planes (dashed lines in map view) are virtually fitted through the two seismic clouds (better illustrated in the inset on the lower left). Note that the orientation of the virtual planes may change with increasing seismicity. The stress orientation derived from borehole breakout and drilling induced tensile fracture analysis indicates the open fractures to be optimally oriented for dilation in domain 3 and slip in domain 4, thus favouring enhanced fracture permeability. Colour coding of the slip tendency (Ts) plot in the insert on the right is from low (blue) to high (red). Note the two crosses in the Ts plot marking the orientation of the two virtual planes, favourably oriented for slip reactivation under reasonable static friction coefficient of 0.8. (For interpretation of the references to colour in this figure legend, the reader is referred to the web version of this article.)

characteristics), and gravity modelling. During project development new observations from well data (especially from image logs) and seismological data were added (Table 1).

Structural reservoir modelling has been performed using the software-package Move2018^{TM} developed and distributed by Midland Valley Exploration Ltd. The structural model represents the backbone of further numerical simulations (fluid flow, thermo-hydraulic, pressure) performed outside of Move.

Polar plots (lower hemisphere) of fracture poles of domains 3 and 4 suggest a general optimal orientation of most of the observed fractures in the in-situ stress field (Figs. 7 and 12). Domain 3 fractures strike mainly sub-parallel to the PTF. A second but subordinate fracture set strikes ENE (NNW dipping) at a high angle to the PTF. Domain 4 fractures are more scattered in orientation and the main trend is slightly rotated counterclockwise with respect to the domain 3 fracture set, as discussed above. With respect to the stress field orientation, the majority of domain 3 fractures are more prone to open in tensile mode, whereas domain 4 fractures are more prone to slip, provided the assumption of a homogeneous stress field is valid.

The events of the upper and lower seismic cluster form elongate clouds aligning along steep dipping virtual planes dipping towards NNE (026°/83° and 026°/71° respectively; Fig. 12), similar to the main trends of domain 3 and 4 open fractures (Fig. 7) but rotated some 20° anticlockwise. The dip angle is similar to the PTF envelope cross-courses, i.e. the Great Eastern and Great Western cross-course (Fig. 11). The dip direction of the virtual plane is 40° off the mean dip direction of the PTF. The upper cluster/plane seems to be within the PTF domain 3, and the lower in the footwall domain 4 (Figs. 11 and 12). Due to insufficient data the structural relation especially of the lower cluster/plane to the PTF is uncertain but fits best to the trends of the open fracture subset.

The Slip-Tendency method calculates the potential reactivation of faults in the prevailing stress field (Morris et al., 1996). For fault reactivation, the critical value of the parameter T_S, which is the ratio of shear stress τ to effective normal stress σ_{neff} across the plane of the fracture in question, is given by the static friction coefficient μ_S ($\mu_S = \tau/\sigma_n$; Byerlee, 1978). Assuming a cohesionless fault, failure (i.e. shear) occurs at $T_S \geq \mu_S$. The greater the ratio τ/σ_{neff} or T_S, the more probable is the reactivation of the fault plane (Morris et al., 1996).

Slip tendency is calculated for arbitrary oriented fractures and plotted color-coded in a polar plot (lower hemisphere) applying the stress observations described above (Fig. 12). Both seismically active virtual planes fall into sections of highest slip tendency.

9. Discussion

The reservoir currently can only be defined through observations of the PTF envelope at surface, along the open hole section of UD-1 and by the induced seismicity. Due to the 4 km separation of the PTF exposures at the surface and along the UD-1 borehole, interpolation is uncertain. Structural data from UD-2 would be helpful in this regard.

Initially, the envisaged reservoir was thought to be the highly fractured volume of the PTF between the Great Eastern and Great Western cross-course (defining the PTF envelope), which is identified as domain 3 in the fracture distribution along the open hole section. Interestingly, the main hydro-mechanical activity as indicated by mud losses during drilling, changes in temperature gradient and induced seismicity (lower cluster) appears to lie mainly outside this domain 3 zone in the footwall of the PTF (domain 4). At this stage of the project there appears therefore to be some inconsistency in defining the reservoir purely by

structure (fracture intensity) or by hydraulic characteristic (e.g. mud losses, gas shows). This is not necessarily surprising given the data limitations and the fact that natural flow systems within the highly fractured and stress-sensitive volume drilled are likely to be highly heterogeneous. Further data, especially from UD-2, and ongoing hydraulic testing should help to reduce these uncertainties.

Minor indications of hydraulically active zones are also present within domain 3, including small changes in temperature gradient (Fig. 10) and induced seismicity (upper cluster). This would correspond to the PTF envelope itself, projected from surface. However, as discussed above, this projection is subject to uncertainty. In particular, large NNW-dipping faults observed at surface south of the site are interpreted as intersecting UD-1 at >3 km and it is possible that they offset or rotate the course of the PTF at depth. Significant faults of this trend are seen in the image log data (Fig. 5).

Additional well testing is currently (winter/spring 2021) ongoing. A well clean-up operation of UD-1 is planned for July 2021.

10. Conclusions

Two deep wells (UD-1 and UD-2) have been successfully drilled into the Carnmenellis granite in Cornwall/UK to be used for geothermal power production. Mud losses observed during drilling, some of which led to induced seismicity, gas shows, post-drilling temperature logs, and initial testing demonstrate that natural permeability exists at >4 km where reservoir temperature is up to 180 °C at 5 km depth.

The encountered fracture reservoir is related to the steeply dipping Porthtowan Fault Zone (PTF), which remains poorly resolved at intermediate depth until wireline logging is undertaken in UD-2. Within the reservoir section of UD-1, a partially open fracture network interpreted from image logs, optimally oriented for dilation or slip to the prevailing in-situ stress field also indicates the existence of porosity in the reservoir. Although many fractures could be identified in the open hole section of UD-1 only a small subset seem to be hydraulically active, serving as primary conduits for fluid flow. Intervals with high fracture frequency do not necessarily correlate with high mud losses or induced seismicity, as often seen in fractured formations. The structural limits of the PTF as implied by fracture intensity statistics do not correlate spatially and orientationally with the most hydraulically active fracture zones.

The monitoring of induced microseismicity during drilling operations has been shown to be useful for early characterisation of the reservoir. However, the observed induced seismicity does not reflect fluid circulation between the two wells (as no circulation test has been performed yet) but only the reservoir behaviour while hydraulic injection testing in UD-1. The deep reservoir section seems to be much more sensitive to injection than the shallower one.

Well productivity / injectivity started at a relatively low level but has been improved through a varied approach to stimulation. The main objective is to enable a safe, clean, sustainable, and economic production of geothermal energy.

This paper is intended to serve as an initial report and benchmark reference for ongoing development of the United Downs Deep Geothermal Project, the first geothermal power project in the UK.

CRediT authorship contribution statement

John Reinecker: Conceptualization, Investigation, Writing – original draft. **Jon Gutmanis:** Conceptualization, Investigation, Writing – review & editing. **Andy Foxford:** Investigation, Writing – review & editing. **Lucy Cotton:** Investigation, Writing – review & editing. **Chris Dalby:** Investigation, Writing – review & editing. **Ryan Law:** Project administration, Resources, Writing – review & editing.

Declaration of Competing Interest

The authors declare that they have no known competing financial interests or personal relationships that could have appeared to influence the work reported in this paper.

Acknowledgements

This work has been supported by the 'Science for Clean Energy' (S4CE) European research consortium and by the project 'Multidisciplinary and multi-context demonstration of Enhanced Geothermal Systems exploration and Exploitation Techniques and potentials' (MEET), both funded by the European Union's Horizon 2020 research and innovation programme under grant agreement No 764810 (S4CE) and No 792037 (MEET). Chris Dalby was supported by NERC iCASE PhD studentship (NE/R008612/1). We thank Geothermal Engineering Limited for permission to publish. We also thank colleagues at GeoScience Limited notably Dr Tony Batchelor and Peter Ledingham for fruitful discussions on the technical issues at United Downs, Gavyn Rollinson and Robin Shail at the University of Exeter for mineralogical analysis and discussions on regional geology, granites and mineralisation, and Kristian Bär (TU Darmstadt) for fruitful discussions during preparation of the manuscript.

Also, we highly appreciate the comments and suggestions by three anonymous reviewers which helped clarifying the paper. The editor David Bruhn is thanked for handling our submission.

References

Alexander, A.C., Shail, R.K., 1995. Late Variscan structures on the coast between Perranporth and St. Ives, Cornwall. Proc. Ussher Soc. 8, 398–404.

Baba, M., Parnell, J., Bowden, S., 2018. The geochemistry of oil in Cornish granites. Pet. Geosci. 25, 298–305.

Batchelor, A.S., Pine, R.J., 1986. The results of in situ stress determinations by seven methods to depths of 2500 m in the Carnmenellis granite. In: Proceedings of the International Symposium on Rock Stress Measurements, Stockholm, 1.-3. September 1986, pp. 467–478.

Beamish, D., Busby, J., 2016. The Cornubian geothermal province: heat production and flow in SW England: estimates from boreholes and airborne gamma-ray measurements. Geotherm. Energy 4 (4). https://doi.org/10.1186/s40517-016-0046-8.

BGS, 1975. British Regional Geology. HMSO, South-West England, 4th edition, 1975.

Bois, C., Cazes, M., Hirn, A., Mascle, A., Matte, P., Montadert, L., Pinet, B., 1988. Contribution of deep seismic profiling to knowledge of the lower crust in France and neighbouring areas. Tectonophysics 145, 253–275.

Brooks, M., Doody, J.J., Al-Rawi, F.R.J., 1984. Major reflectors beneath SW England. J. Geol. Soc. 141, 97–103.

Byerlee, J.D., 1978. Friction of rocks. Pure Appl. Geophys. 116, 615–626.

Carstens, P., Wittmann, K., 2019a. Report within Horizon 2020 project "S4CE", released on 17th April 2019, p. 11.

Carstens, P., Wittmann, K., 2019b. Report within Horizon 2020 project "S4CE", released on 2nd July 2019, p. 4.

Charoy, B., 1986. The Genesis of the Cornubian Batholith (South-West England): the example of the Carnmenellis Pluton. J. Petrol. 27, 571–604.

Chen, Y., Zentilli, M.A., Clark, A.H., Farrar, E., Grist, A.M., Willis-Richards, J., 1996. Geochronological evidence for post-Variscan cooling and uplift of the Carnmenellis granite, SW England. J. Geol. Soc. 153, 191–195.

Chesley, J.T., Halliday, A.N., Snee, L.W., Mezger, K., Shepherd, T.J., Scrivener, R.C., 1993. Thermochronology of the Cornubian batholith in SW England: Implication for pluton emplacement and protracted hydrothermal mineralization. Geochim. Cosmochim. Acta 57, 1817–1835.

Cotton, L., 2016. Realising the Potential of Geothermal Energy in Cornwall - Locating Sites for Future Production. Unpublished master thesis. University College, Cork, Ireland, p. 82.

Faulkner, D.R., Mitchell, T.M., Rutter, E.H., Cembrano, J., 2008. On the structure and mechanical properties of large strike-slip faults In: The Internal Structure of Fault Zones: Implications for Mechanical and Fluid Flow Properties, Eds., 299. Geological Society London Special Publication, pp. 139–150.

GeoScience Ltd, 2009. Unpublished report to Geothermal Engineering Limited.

Holloway, S., Chadwick, R.A., 1986. The Sticklepath-Lustleigh fault zone: Tertiary sinistral reactivation of a Variscan dextral strike-slip fault. J. Geol. Soc. 143, 447–452.

Jones, R.H., 1991. A seismic reflection survey as part of a geophysical investigation of the Carnmenellis Granite. Proc. Ussher Soc. 7, 418–420.

Kim, Y.S., Andrews, J.R., Sanderson, D.J., 2001. Extension fractures, secondary faults and segment linkage in strike-slip fault systems at Rame Head, Southern Cornwall. Geosci. SW Engl. 10, 123–133. Proceedings of the Ussher Society.

LeBoutillier, N.G., 2002. The Tectonics of Variscan Magmatism and Mineralisation in Southwest England. Doctoral thesis. University of Exeter, p. 712.
Lemiszki, P.J., Brown, L.D., 1988. Variable crustal structure of strike-slip fault zones as observed on deep seismic reflection profiles. Bull. Geol. Soc. Am. 100, 665–676.
Leveridge, B.E., Holder, M.T., Goode, A.J.J., 1990. Geology of the country around Falmouth. In: Memoir of the British Geological Survey, Sheet 352 (England and Wales).
Leveridge, B.E., Hartley, A.J., 2006. The Variscan Orogeny: the development and deformation of Devonian/Carboniferous basins in SW England and South Wales. In: Brenchley, P.J., Rawson, P.F. (Eds.), The Geology of England and Wales, Eds. Geological Society of London, pp. 225–255.
Martel, S.J., 1990. Formation of compound strike-slip fault zones, Mount Abbot quadrangle, California. J. Struct. Geol. 12, 869–882.
Massart, B., Paillet, M., Henrion, V., Sausse, J., Dezayes, C., Genter, A., Bisset, A., 2010. Fracture characterization and stochastic modeling of the granitic basement in the HDR soultz project, France. In: Proceedings World Geothermal Congress, Bali, Indonesia, April 25-29, 2010.
Morris, A.P., Ferrill, D.A., Henderson, D.B., 1996. Slip tendency and fault reactivation. Geology 24, 275–278.
Parker, R., 1989. Hot Dry Rock: Geothermal Energy: Phase 2B Final Report of the Camborne School of Mines Project. Pergamon Press, p. 1096.
Parker, R., 1999. The Rosemanowes HDR project 1983–1991. Geothermics 28, 603–615.
Pine, R.J., Batchelor, A.S., 1984. Downward migration of shearing in jointed rock during hydraulic injections. Int. J. Rock Mech. Mining Sci. Geomech. Abstr. 21 (5), 249–263.
Pine, R.J., Tunbridge, L.W., Kwakwa, K.A., 1983a. In-situ stress measurement in the Carnmenellis granite –I. Overcoring tests at South Crofty mine at a depth of 790 m. Int. J. Rock Mech., Mining Sci. Geomech. Abstr. 20 (2), 51–62.
Pine, R.J., Ledingham, P., Merrifield, C.M., 1983b. In-situ stress measurement in the Carnmenellis granite –II. Hydrofracture tests at Rosemanowes quarry to depths of 2000 m. Int. J. Rock Mech. Min. Sci. Geomech. Abstr. 20 (2), 63–72.
Rothert, E., 2019. Unpublished report to Geothermal Engineering Ltd, p. 9.
Simons, B., Shail, R.K., Andersen, J.C., 2016. The petrogenesis of the early permian Variscan granites of the cornubian batholith: lower plate post-collisional peraluminous magmatism in the Rhenohercynian Zone of SW England. Lithos 260, 76–94.
Taylor, G.K., 2007. Pluton shapes in the Cornubian batholith: New Perspectives from Gravity modelling. J. Geol. Soc. 164, 525–552.
Warr, L.N., Primmer, T.J., Robinson, D., 1991. Variscan very low-grade metamorphism in southwest England: a diastathermal and thrust related origin. J. Metamorph. Geol. 9, 751–764.
Willis-Richards, J., Jackson, N.J., 1989. Evolution of the Cornubian ore field, Southwest England; Part I, Batholith modeling and ore distribution. Econ. Geol. 84, 1078–1100.
Willis-Richards, J., 1990. Thermotectonics of the Cornubian batholith and their Economic significance. Ph.D. thesis. Camborne School of Mines, UK.
Willis-Richards, J., 1995. Assessment of HDR reservoir stimulation and performance using simple stochastic models. Geothermics 24, 385–402.